THE ASTROPHYSICAL JOURNAL, 427:L75–L78, 1994 June 1

MEASUREMENT OF THE SUNYAEV-ZEL'DOVICH EFFECT TOWARD ABELL 2163 AT A WAVELENGTH OF 2.2 MILLIMETERS

T. M. WILBANKS,[1] P. A. R. ADE,[2] M. L. FISCHER,[1] W. L. HOLZAPFEL,[1] AND A. E. LANGE[1]

Received 1993 January 25; accepted 1994 March 16

ABSTRACT

We report the first significant detection of the Sunyaev-Zel'dovich (S-Z) effect at millimeter wavelengths. Drift scans of the cluster of galaxies Abell 2163 were performed using a novel bolometric array receiver at a wavelength of 2.2 millimeters. The measured decrement in sky brightness corresponds to a peak Comptonization of the cosmic microwave background radiation at the cluster of center $y = (3.78^{+0.74}_{-0.65}) \times 10^{-4}$. Measurements at millimeter wavelengths are necessary to separate the thermal and kinetic S-Z effects. The value of the Hubble constant can be derived from the amplitude of the thermal effect in combination with the measured X-ray properties of the cluster. The radial peculiar velocity of the cluster relative to its local CMB rest frame can be derived from the relative amplitude of the kinetic and thermal effects and the X-ray temperature.

Subject headings: cosmic microwave background — cosmology: observations — galaxies: clusters: individual (A2163) — instrumentation: detectors

1. INTRODUCTION

The distortion of the spectrum of the cosmic microwave background (CMB) due to Compton scattering by the hot electron gas of the intergalactic medium in a cluster of galaxies was first suggested by Sunyaev & Zel'dovich (1972) and has recently been reviewed by Rephaeli & Lahav (1991). There are two Sunyaev-Zel'dovich (S-Z) effects: a thermal effect due to the thermal motion of the electrons in the gas and a kinetic effect due to the peculiar velocity of the gas with respect to the CMB. The thermal effect produces a decrease in the CMB brightness at wavelengths longer than $\lambda = 1.38$ mm, and an increase in brightness at shorter wavelengths. The amplitude of the thermal effect is proportional to the Compton parameter $y = \int \sigma_T n_e T_e dl$, where σ_T is the Thomson cross section, n_e is the electron density, $T_e = kT/(m_e c^2)$ is the dimensionless electron temperature, and dl is the line of sight through the cluster. In the Rayleigh-Jeans portion of the spectrum the decrease in CMB temperature is given by $\Delta T_{CMB}/T_{CMB} = -2y$.

The kinetic effect is a Doppler shift, and corresponds to a temperature variation $\Delta T_{CMB}/T_{CMB} = 2(v_r/c) \int \sigma_T n_e dl$, where v_r is the radial component of the peculiar velocity of the cluster. For typical cluster temperatures and peculiar velocities $\lesssim 5 \times 10^3$ km s^{-1}, the thermal effect will dominate the kinetic effect except at wavelengths close to 1.38 mm. The apparent brightness of each of the S-Z effects is independent of redshift.

A decrease in the brightness of the CMB has been observed at centimeter wavelengths in the direction of several clusters using single dish (Birkinshaw 1991; Klein et al. 1991) and interferometric (Jones et al. 1993) measurements. These measurements have been combined with the measurements of X-ray properties of the cluster to deduce the value of the Hubble constant, under the assumption that the kinetic effect makes a negligible contribution (Birkinshaw, Hughes, & Arnaud 1992).

Measurements of the S-Z effect at wavelengths near the null of the thermal effect are necessary to separate the thermal and kinetic effects. They have proven to be difficult. Atmospheric noise at millimeter wavelengths can limit sensitivity even when using sophisticated strategies relying on multifrequency receivers and several levels of differencing on the sky (Meyer, Jefferies, & Weiss 1983). Modulation of the beam in the presence of the large thermal background from the telescope can produce large offsets that are dependent on telescope position (Chase et al. 1987). These problems have limited the sensitivity of millimeter-wave measurements to $\Delta y = 1\text{–}2 \times 10^{-4}$. No significant millimeter-wavelength detections have previously been made.

The detection described in this paper was made in the direction of the rich Abell cluster A2163, an unusually X-ray bright cluster at redshift $z = 0.2$ (Arnaud et al. 1992). The observing strategy used reduces or eliminates many of the problems present in earlier attempts to observe S-Z at millimeter wavelengths.

2. INSTRUMENTATION

Observations were made at the Caltech Submillimeter Observatory (CSO) on Mauna Kea using a 2×3 array of bolometric detectors operated at 300 mK. The small array was designed to test a novel scheme for obtaining the difference signal between pairs of pixels in the array electronically, without optical modulation.

A detailed description of the instrument will be presented elsewhere (Wilbanks et al. 1994). A tertiary mirror images the telescope's Cassegrain focus into the receiver. The aperture of a 2 K Lyot stop subtends 50% of the primary mirror area. A 2×3 array of parabolic concentrators couples the radiation from the tertiary focal surface to the bolometric detectors. The concentrators are oriented toward the center of the Lyot stop, illuminating the center of the primary mirror. The concentrators and bolometers are cooled to 300 mK. The system produces two rows of three collinear beams with 2'.2 center-to-center spacing on the sky between adjacent pixels. The beams have near Gaussian shape, with a 1'.4 FWHM.

The spectral response of the six elements in the array is determined by a common set of filters located between the Lyot stop and the entrance aperture of the cones. Multilayer metal-mesh filters define a band centered at 2.2 mm with a width $\Delta\lambda/\lambda = 0.11$ FWHM. This band includes the peak brightness of the decrement in the thermal effect, and is

[1] Department of Physics, University of California, Berkeley, CA 94720.
[2] Physics Department, Queen Mary and Westfield College, Mile End Road, London E1 4NS, UK.

designed to maximize the ratio of $I_{SZ}/I_{atmosphere}$. The spectral response of each array element was measured in the laboratory, indicting only minor variations between elements.

The electronic differencing scheme is described in detail by Rieke et al. (1989), Wilbanks et al. (1990), and Devlin et al. (1991). Each set of three detectors (Alsop et al. 1992) is well matched in electrical and thermal properties. The difference signal between each pair of detectors is obtained in an AC bridge. The output of each bridge is amplified and phase-synchronously demodulated, producing a stable DC signal proportional to the difference in power absorbed on the two detectors. Each bridge is trimmed to null the response to common-mode changes in atmospheric emission (Glezer, Lange, & Wilbanks 1992). For atmospheric emission, the system is equivalent to a square wave chop between the two beams at infinite frequency.

Three difference signals (one with 4.'3 beam separation and two with 2.'2 beam separation) are obtained for each row by placing each of the three possible pairs of detectors in a separate bridge. The output of each bridge is filtered with a four-pole low-pass filter set at 2.25 Hz and digitally sampled at 5 Hz. Observations are performed by fixing the telescope in position and using the Earth's rotation to drift the source across a row of detectors as shown in Figure 1. The row is kept parallel to the direction of the drift scan over the course of the observation by rotating the array about the optical axis between scans. Keeping the telescope fixed with respect to Earth during each scan eliminates sensitivity to position-dependent offsets.

3. OBSERVATIONS

We observed Abell 2163 (A2163, R.A. = $16^h13^m06^s$, $\delta = -06°01'20''$, J1950) on the nights of 1993 April 24–26 for a total of 16 hr of integration at zenith angles between 25° and 50°. The optical depth of the atmosphere at 2.2 mm was less than 0.08 for observations of planetary calibrators and was less than 0.04 for observations of A2163, and has been corrected for in all cases.

In order to provide a test for baseline artifacts, we began alternate scans at one of two right ascension offsets (RAOs), defined as the distance in R.A. between the source and the center of the array at the beginning of the scan. On April 24, we accumulated 109 scans, each 34′ (136 s) in length with the RAO alternating between 16.'5 and 22.'5. The declination of the array was such that the 3 pixels designated row 1 drifted directly over the X-ray center of the source, while the other 3 pixels, designated row 2, were offset 2.'2 north in declination. On April 25 and 26 we accumulated 162 and 161 scans, respectively, each 26′ (104 s) long, with the RAO alternating between 8.'5 and 14.'5. On April 25, row 1 was centered on the source, with row 2 2.'2 to the north; on April 26 row 2 was centered on the source, with row 1 2.'2 to the south. There are thus 12 data sets in total: two RAO offsets of two rows on each of three nights.

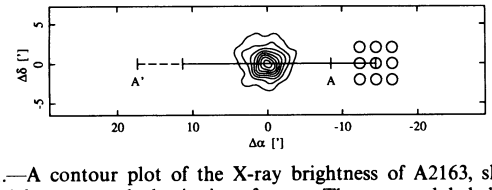

FIG. 1.—A contour plot of the X-ray brightness of A2163, showing the position of the array at the beginning of a scan. The axes are labeled in position offset from the position of the peak of the X-ray emission ($\alpha = 16^h13^m06^s$, $\delta = 6°01'20''$, J1950). Each contour corresponds to $5\gamma\ s^{-1}\ arcmin^{-2}$ (in excess of 3 σ). The X-ray brightness profile FWHM = 2.'3. The calculated SZ brightness profile (see text) is broader, with FWHM = 5.'2. During each scan, one of the two rows in the array was placed at the declination of the X-ray centroid, with the other row 2.'2 either north or south, resulting in the coverage shown. The array is shown at the beginning of a 14.'5 RAO scan, which extends along the solid bar. Scans with 8.'5 RAO proceed from A to A′.

4. CALIBRATION

Scans of Jupiter, Saturn, and Mars were made in order to map the beam shapes of the array and to calibrate the system responsivity. The beam shape changed slightly in a reproducible fashion as the array was rotated about the optical axis. During observations of A2163 the rotation of the array relative to the horizon ranged from −60° to 60°. Because we do not have sufficient data to derive a model for the variation of beam shape with angle, we determined an average calibration for each night. We estimate a ±6% uncertainty in the calibration of the difference signals due to variations in system responsivity and variations in the signal template (described below) resulting from changes in beam shape. In addition, we assign a ±5% uncertainty in the brightness of the primary calibrator, Mars (Ulrich 1981). Finally, since the spectrum of Mars is different from that of an S-Z source, there is a ±2% uncertainty in the calibration of the difference signals due to the variation in spectral response between array elements. Overall, the system calibration has an uncertainty of ±8%.

5. ANALYSIS

A source produces a signal with a characteristic temporal shape as it drifts through the positive and negative beams of each difference. The shape of the signal depends on the separation and shapes of the beams and, if the source is extended, on the morphology of the source and the offset in declination between the source and the beams. In order to determine the brightness of A2163, we fitted the data to a signal template that is calculated from the measured beam shapes and separations and from a calculated source morphology for the S-Z effect in A2163. The morphology of the S-Z effect in A2163 is calculated from its X-ray morphology under the assumption that the distribution of the plasma is described by an isothermal sphere, implying surface brightness $\Sigma = \Sigma_0[1 + (r/R_0)^2]^{-3\beta+1/2}$. Arnaud et al. (1992) find that the X-ray morphology of A2163 is well fitted by a core radius $R_0 = 1.'15$ (−0.32, +0.39) and $\beta = 0.59$ (−0.06, +0.08) (90% confidence limits). The S-Z brightness profile calculated using these parameters has a FWHM of 5.'2, and is thus significantly extended with respect to the 1.'4 beam. The signal template for each of the three differences in each of the rows is calculated by convolving the S-Z brightness profile at the appropriate declination with the measured beam profiles (Fig. 2).

The data is cleaned of transients due to cosmic rays and then binned into 3.2 s intervals corresponding to 0.'8 along the scan direction. The best-fit signal amplitude is found for each scan by fitting the binned data to the sum of an offset, gradient, and the appropriate signal template. The offset and gradient remove linear drifts in the system offset over the period of a scan. For each scan, the three differences in each row are fitted simultaneously to three offsets and gradients and one signal amplitude. Changes in weather conditions produce low-frequency noise of varying amplitude in the data, preventing the construction of a meaningful χ^2 test of the model's goodness of fit to the individual scans.

The signal amplitude and standard error for each of

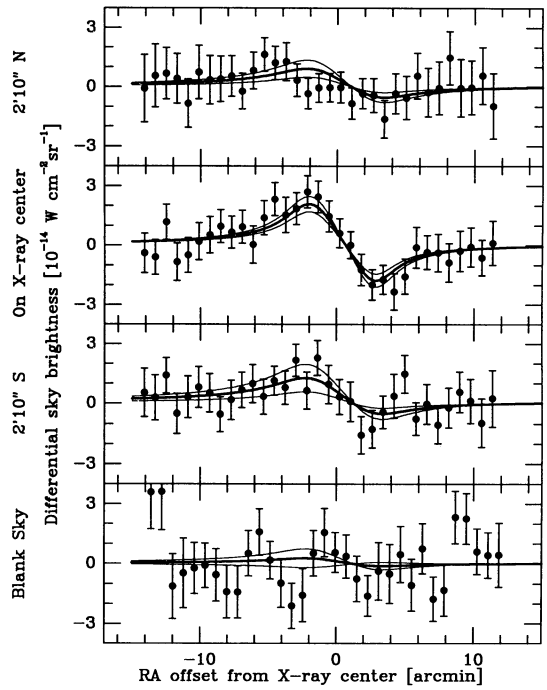

FIG. 2.—Difference signals from scans of A2163 at the three declinations shown in Fig. 1, and from blank sky. The four panels correspond to the 4.'3 difference on A2163 at the 14.'5 RAO for April 25 (*top*) and April 26 (*upper and lower middle*), and to the 4.'3 difference on blank sky at the 14.'0 RAO on April 26. The data shown constitute 3/36 of the total data in all 12 sets of A2163. The best-fit signal template (see text) for each of the data sets is shown by the heavy curve, and has been fit to all three differences, including the two 2.'2 differences not shown. The amplitudes and $\pm 1\ \sigma$ uncertainties (indicated by the light curves) correspond to the values given in Tables 1 and 2. The vertical axis is the brightness of a source that fills one beam completely and fills none of the other beam.

the 12 data sets are found by taking the weighted average of the best-fit amplitudes for all the scans in the data set (Table 1). All of the scans from all the nights are used weighted by σ_i^{-2}, the dispersion of the binned data in the ith scan about the best-fit offset and gradient. Since the amplitude of the signal due to astrophysical sources is small in any one scan, σ_i is a good measure of the amplitude of noise in that scan. The measured signal amplitude typically changes by $\pm 5\%$ if an unweighted average is taken.

The value quoted for y (Table 1) refers to the signal that would be measured by a pencil beam observation toward the center of the isothermal gas distribution used to calculate the model signal.Our experiment's finite beam size and separation dilute the measured signal amplitude of A2163 to 16% and 35% (2.'2 and 4.'3 separations) of this value. The weighted mean of all of the observations yields a best-fit value of $y = 3.78 \pm 0.35 \times 10^{-4}$, corresponding to a maximum decrement in brightness at the cluster center of $\nu I_\nu = 5.7 \times 10^{-14}$ W cm^{-2} sr^{-1}. The distribution of the 12 individual measurements has a $\chi^2 = 8.6$ for 11 d.o.f. (65% probability range is 6.8–14.9).

The similarity between the best-fit values for y for the three declination offsets indicates that the morphology that we have assumed for the S-Z source is a good approximation. We have repeated the entire analysis varying the values of the parameters R_0 and β in order to understand the sensitivity of y to the assumed morphology. Over the range of values of R_0 and β that lie within the 90% confidence limits quoted by Arnaud et al. (1992) the measured value of y ranges from 4.32 ± 0.39 ($R_0 = 0.83$, $\beta = 0.53$) to 3.37 ± 0.31 ($R_0 = 1.54$, $\beta = 0.67$). The $1\ \sigma$ uncertainty in y due to the uncertainty in the parameters describing the isothermal sphere source model is thus comparable to the statistical uncertainty of our measurement.

Our analysis assumes that the S-Z brightness centroid is coincident with the X-ray brightness centroid. If it is not, then we will systematically underestimate y. The consistency between the values of the peak central decrement derived from the scans through the X-ray centroid and from the scans offset 2.'2 to the north and south indicates that there is no significant offset in declination.

The R.A. of the S-Z centroid can be determined by finding the best-fit source position along the scan. The signal to noise is too low to allow the source position to be a free parameter in the fits to individual scans. However, a best-fit R.A. can be determined for each of the 12 data sets by averaging all of the scans within a data set before fitting the signal templates. After removing offsets and linear gradients for each of the three differences, all of the scans in each data set are averaged, weighted by σ_i^{-2}. Three of the resulting 36 average differences, corresponding to the 4.'3 beam separation for one night at one offset at declination offsets of $+2.'2$, $0'$, and $-2.'2$ are shown in Figure 2. The appropriate signal template is fitted to each difference, and the χ^2 of the residuals for all three differences in a row is minimized simultaneously constraining the amplitude and R.A. of the source to be the same for all three differences. The best-fit signal templates for each of the data sets in Figure 2 is shown by the heavy curve, with the $\pm 1\ \sigma$ uncertainty in amplitude indicated by the light curves.

The amplitudes found for each of the twelve data sets using the procedure are consistent with those found by the scan by scan fitting procedure. The best-fit R.A. of the S-Z centroid is within 1.'0 of the X-ray centroid for the eight data sets that have detections at more than 95% confidence. The weighted average of the source position is $-0.'06 \pm 0.'16$ from the X-ray centroid.

TABLE 1

BEST-FIT CENTRAL S-Z EFFECT FOR A2163

Date (1993)	Right Ascension Offset	$\Delta\delta = 0'$ (10^{-4} y)	$\Delta\delta = +2'10''$ (10^{-4} y)	$\Delta\delta = -2'10''$ (10^{-4} y)
Apr 24	16.'5	2.65 ± 1.59	4.78 ± 2.03	...
	22.5	2.65 ± 1.46	1.31 ± 1.95	...
Apr 25	8.5	4.34 ± 0.96	4.99 ± 1.76	...
	14.5	2.36 ± 0.99	2.80 ± 1.52	...
Apr 26	8.5	4.86 ± 0.76	...	3.50 ± 1.59
	14.5	4.17 ± 0.77	...	3.48 ± 1.62
Weighted mean	...	3.89 ± 0.40	3.43 ± 0.89	3.49 ± 1.14

There is no evidence of a significant offset in R.A. between the X-ray and S-Z brightness profiles.

It is unlikely that there are artifacts in the baseline due to modulation of emission from warm sources, since the telescope is fixed in position during each of the scans. It is possible, however, that the motion of the telescope between scans produces a fluctuation in the receiver offset that is synchronous with the scan period. We test for this possibility by looking for a significant variation in the signal amplitude with RAO, and by searching for a signal in data obtained on blank sky.

While the difference in the amplitudes found in the short and long RAO observations is marginally significant (1.5 σ), the blank sky data show no evidence for a baseline artifact that would significantly affect the measured amplitude. We accumulated 6.7 hr of integration on a patch of sky void of known sources. The data were collected over the same range of hour angle and zenith angle and analyzed in the same way as for A2163, except that each row was assumed to be centered on the source. The results are summarized in Table 2. The average of the blank sky measurements is $y = 0.24 \pm 0.41 \times 10^{-4}$. We assign the uncertainty due to systematic effects in the baseline to be the 1 σ uncertainty in the blank sky measurements. The overall uncertainty of the measurement is taken to be the quadrature sum of the statistical uncertainty of the single scan fits, the calibration uncertainty, and the baseline uncertainty. This gives an overall result of $y = 3.78 \pm 0.62 \times 10^{-4}$. When the uncertainty in the parameters that characterize the isothermal sphere model is included $y = (3.78^{+0.74}_{-0.65}) \times 10^{-4}$.

TABLE 2

BEST-FIT CENTRAL S-Z EFFECT FOR BLANK SKY

Date (1993)	Right Ascension Offset	$\Delta\delta = +1'05''$ (10^{-4} y)	$\Delta\delta = -1'05''$ (10^{-4} y)
Apr 24	16.0	0.35 ± 1.36	2.13 ± 2.54
	22.0	-0.25 ± 1.11	-0.37 ± 2.55
Apr 25	8.0	1.53 ± 1.36	-0.32 ± 2.16
	14.0	0.45 ± 1.23	-0.50 ± 2.36
Apr 26	8.0	-1.05 ± 1.21	-0.07 ± 1.59
	14.0	0.46 ± 1.05	0.49 ± 1.13
Weighted mean	...	0.23 ± 0.49	0.25 ± 0.73

6. DISCUSSION

Although astrophysical confusion from randomly distributed sources is expected to be small at millimeter wavelengths (Fischer & Lange 1993), the possibility of confusion due to sources associated with the cluster must be carefully considered in any measurement of the S-Z effect. The amplitude of anisotropic interstellar dust emission calculated from the *IRAS* 100 μm map and scaled with the sky-average spectrum of dust emission (Wright et al. 1991), is negligible. A recent VLA search toward A2163 shows evidence of a radio source 0.8 west of the cluster center with an inverted spectrum (Herbig & Birkinshaw 1992). For this source the flux rises from 1 to 3 mJy between 6 and 2 cm, suggesting a flux as large as 30 mJy at 2.2 mm, corresponding to $y = -1.8 \times 10^{-4}$ for our system. However, Fischer & Radford (1993) report an upper limit of 5 mJy (2 σ in a 20″ Decl., 10″ R.A. beam) on point source emission within 1′ of the X-ray center at a wavelength of 3.3 mm. A 5 mJy point source at 2.2 mm corresponds to a y parameter of -0.3×10^{-4} for our system. We conclude that there are no significant celestial sources of contamination in the vicinity of our observation.

Another source of confusion to measurements of the thermal S-Z effect is the kinetic S-Z effect. The ratio of the amplitudes of the kinetic and thermal effects at 2.2 mm is I_k/I_t (2.2 mm) = 0.143 $(v_{\rm pec}/1000\ {\rm km\ s^{-1}})$ $(T_e/10\ {\rm keV})^{-1}$, 1.7 times larger than the long wavelength limit (Arnaud et al. give an electron temperature, $T_e = 13.8$ keV for A2163). The kinetic effect would contribute significantly in our 2.2 mm band only for large values of the peculiar velocity of the cluster.

The values that we quote for y in this paper assume that the kinetic S-Z effect is zero. Additional measurements at $\lambda \leq 1.38$ mm are necessary in order to measure the kinetic contribution to the quoted y parameter. We have obtained measurements at 1.2 mm. The results of these measurements, and estimates of H_0 and the cluster peculiar velocity derived from the 1.2 and 2.2 mm measurements will be presented in a future paper.

7. CONCLUSIONS

We have made the first significant detection of the S-Z effect at millimeter wavelengths, using a novel bolometric receiver and drift-scan observations. The measured amplitude of the central decrement corresponds to $y = (3.78^{+0.74}_{-0.65}) \times 10^{-4}$. The sensitivity of this technique is adequate to provide a high S/N measurement of the amplitude of the thermal S-Z effect on the X-ray bright cluster A2163 in a single night of integration. Baseline artifacts and astrophysical confusion make negligible contributions to the measured decrement.

This work has been made possible by a grant from the David and Lucile Packard Foundation, and by a National Science Foundation Presidential Young Investigator award to A. E. L. S. Grannan, T. Hirao, T. Ho, and D. Osgood each made important contributions to this project. We thank J. Keene and G. Serebyn for providing the tertiary optics used at the CSO, and A. Schinckel and the entire staff of the CSO for their excellent support during the observations. The CSO is operated by the California Institute of Technology under funding from the National Science Foundation, Contract No. AST 90-15755.

REFERENCES

Alsop, D. C., Inman, C., Lange, A. E., & Wilbanks, T. 1992, Appl. Opt., 31, 6610
Arnaud, M., Hughes, J. P., Forman, W., Jones, C., Lachieze-Rey, M., Yamashita, K., & Hatsukade, I. 1992, ApJ, 390, 345
Birkinshaw, M. 1991, in Physical Cosmology, ed. A. Blanchard et al. (Gif-sur-Yvette: Editions Frontières), 177
Birkinshaw, M., Hughes, J. P., & Arnaud, K. A. 1991, ApJ, 379, 466
Chase, S. T., Joseph, R. D., Robertson, N. A., & Ade, P. A. R. 1987, MNRAS, 225, 171
Devlin, M., Lange, A. E., Wilbanks, T., & Sato, S. 1993, IEEE Trans. Nucl. Sci., 40, 162
Fischer, M. L., & Lange, A. E. 1993, ApJ, 419, 194
Fischer, M. L., & Radford, S. 1993, private communication
Glezer, E. N., Lange, A. E., & Wilbanks, T. M. 1992, Appl. Opt., 31, 7214
Herbig, T., & Birkinshaw, M. 1992, private communication
Jones, M., et al. 1993, Nature, 365, 322
Klein, U., Rephaeli, Y., Schlickeiser, R., & Wielebinski, R. 1991, Astr. Ap., 244, 43
Meyer, S. S., Jefferies, A. D., & Weiss, R. 1983, ApJ, 271, 1
Rephaeli, Y., & Lahav, O. 1991, ApJ, 372, 21
Rieke, F. M., Lange, A. E., Beeman, J. W., & Haller, E. E. 1989, IEEE Trans. Nucl. Sci., 36, 946
Sunyaev, R. A., & Zel'dovich, Ya. B. 1972, Comments Astrophys. Space Phys., 4, 173
Ulich, B. L. 1981, Astron. J., 86, 1619
Wilbanks, T., Devlin, M., Lange, A. E., Sato, S., Beeman, J. W., & Haller, E. E. 1990, IEEE Trans. Nucl. Sci., 37, 566
Wilbanks, T., et al. 1994, in preparation
Wright, E. L., et al. 1991, ApJ, 381, 200